Available online at www.sciencedirect.com
SCIENCE DIRECT®
Bioorganic & Medicinal Chemistry
ELSEVIER
Bioorganic & Medicinal Chemistry 12 (2004) 4791–4801

A highly bioactive lignophenol derivative from bamboo lignin exhibits a potent activity to suppress apoptosis induced by oxidative stress in human neuroblastoma SH-SY5Y cells

Yukihiro Akao,[a,*] Norio Seki,[b] Yoshihito Nakagawa,[a] Hong Yi,[a] Kenji Matsumoto,[a] Yukie Ito,[c] Kuniyasu Ito,[b] Masamitu Funaoka,[d] Wakako Maruyama,[e] Makoto Naoi[a] and Yoshinori Nozawa[a]

[a]*Gifu International Institute of Biotechnology, Kakamigahara, Gifu 504-0838, Japan*
[b]*Gifu Prefectural Human Life Technology Research Institute, Takayama, Gifu 506-0058, Japan*
[c]*Aichi-Konan college, Konan, Aichi 483-8086, Japan*
[d]*Faculty of Bioresources, Mie University, Tsu, Mie 514-8507, Japan*
[e]*National Institute of Longevity Sciences, Obu, Aichi 474-8522, Japan*

Received 13 May 2004; revised 9 July 2004; accepted 9 July 2004
Available online 6 August 2004

Abstract—Approaches to protection against neurodegenerative diseases, in which oxidative stress and inflammation are implicated, should be based on the current concept on the etiology of these diseases. Recently, a new therapeutic strategy has been proposed to protect neurons from cell death by attenuating the apoptotic signal transduction. Lignin, a durable aromatic network polymer second to cellulose in abundance, was able to be converted into highly active lignophenol derivatives with antioxidant activity by using our newly developed phase-separation technique. These lignophenol derivatives were found to show the potent neuroprotective activity against oxidative stress. Among the compounds examined, a lignocresol derivative from bamboo (lig-8) exhibited the most potent neuroprotective activity against hydrogen peroxide (H_2O_2)-induced apoptosis in human neuroblastoma cell line SH-SY5Y by preventing the caspase-3 activation via either caspase-8 or caspase-9. Furthermore, it was found that lig-8 exerted the antiapoptotic effect by inhibiting dissipation of the mitochondrial membrane permeability transition induced by H_2O_2 or by the peripheral benzodiazepin receptor ligand PK11195. Lig-8 was also shown to be potent in the antioxidant activity in the cells exposed to H_2O_2, as assessed by flow cytometry using 5-(and-6)-chloromethyl-2′,7′-dichlorodihydrofluorescein diacetate and in vitro reactive oxygen species-scavenging potency. These data suggest that lig-8 is a promising neuroprotector, which affects the signaling pathway of neuronal cell death and that it would be of benefit to delay the progress of neurodegenerative diseases.

1. Introduction

The plant cell wall is a complicated semi-interpenetrating network structure built up from cellulose, hemicellulose, and lignin. Lignin is a durable aromatic network polymer second to cellulose in natural abundance. However, the utilization of lignin has not yet been successfully achieved, because lignin molecules lack stereoregularity and also the repeating units in the molecule are heterogeneous and complex. In addition, lignocellulosics components cannot be separated by the simple extraction processes because of nonselective modifications during the drastic isolation process such as the pulping processes, which make lignin molecules even more heterogeneous.

Recently, a new phase-separation system for production of functional lignin derivatives from native lignins was devised.[1,2] This system utilizes phenols and concentrated acid. The resulting lignin derivatives, lignophenols, have highly phenolic function, high stability, and less heterogeneous compared with those after the conventional lignin preparations. The phenolic properties of lignophenols can be modulated by using different phenols.[3] Thus, it can be assumed that the lignophenols derived

Keywords: Lignophenols; Antioxidant; Oxidative stress; Neuronal cell death; Neuroprotection.
* Corresponding author. Tel.: +81-583-71-4646; fax: +81-583-71-4412; e-mail: yakao@giib.or.jp

0968-0896/$ - see front matter © 2004 Elsevier Ltd. All rights reserved.
doi:10.1016/j.bmc.2004.07.022

from native lignins have different phenolic functionalities to exhibit various biological activities. Moreover, the functionality of lignophenols is able to be easily modulated by various modifications.[4]

The antihuman immunodeficiency virus activity of lignins such as lignosulfonate isolated by pulping processes[5] and lignin-like substance extracted from lignocellulosics,[6] and anticancer activity of lignin F[7] have been previously reported. However, these lignins can hardly be used as medicinal resources, because they cannot be mass-produced practically and their molecules are highly heterogeneous.

Apoptosis is an active, energy-dependent process through which living cells initiate their own death, and it is induced by a variety of physiological and pharmacological stimuli. Some clinical evidences show that disturbed apoptotic cell death is associated with certain diseases, such as cancers and immuno-insufficiencies. On the other hand, apoptosis is now considered to be the major death mode of neurons in neurodegenerative disorders such as Parkinson's disease (PD), Alzheimer's disease, and Huntington's disease.[8] In PD, apoptotic features of dopaminergic neurons were detected in the substantia nigra of brains by the terminal deoxylnucleotidyl transferase-mediated nick end labeling method or by electromicroscopic study.[9]

Previous studies have indicated that the neuronal toxicity is mediated and enhanced by reactive oxygen species (ROS) or reactive nitrogen species (RNS) and thus that the oxidative stress accelerates the cell death of neuronal cells in neurodegenerative disorders.[10,11] In fact, such neuronal cell death has been reported to be attenuated by antioxidants and free radical scavengers.[12,13] Recent studies have shown that green tea polyphenols reduced free radical-induced lipid peroxidation.[12] Tea polyphenols have been attracting increasing interest because of their antioxidant, anti-inflammatory,[14,15] anticarcinogenic,[16,17] and iron chelating properties,[18] as demonstrated both in vivo and in vitro. In addition to such properties, these compounds can penetrate the blood–brain barrier,[19] and so may be promising for the development of drugs for treatment or prevention of neurodegenerative diseases associated with oxidative stress. In the present study, we have demonstrated the preventive effect of a highly bioactive lignophenol on the cell death induced by oxidative stress, and also showed that its neuroprotective activity was due to inhibition of caspase activation, prevention of dissipation of the mitochondrial membrane permeability transition (PT), and ROS- or RNS-scavenging activity.

2. Results and discussion

2.1. Characteristics of lignophenol derivatives

Native lignins with complicated 3-dimensional structures were converted to lignophenols by the phase-separation system, the summary of which is given in Figure 1. Lignophenols retain the original interunit linkages formed by dehydrogenative polymerization during the biosynthesis of native lignin, and have high phenolic functionality. By using different phenols for the phase-separation system, the different kinds of lignophenols were produced. Lignopolyphenols, such as lignocatechol, lignoresorcinol, and lignopyrogallol, which have many phenolic hydroxyl groups, are highly hydrophilic. On the other hand, lignomonophenols combined with monohydric phenols such as cresol are water-insoluble.

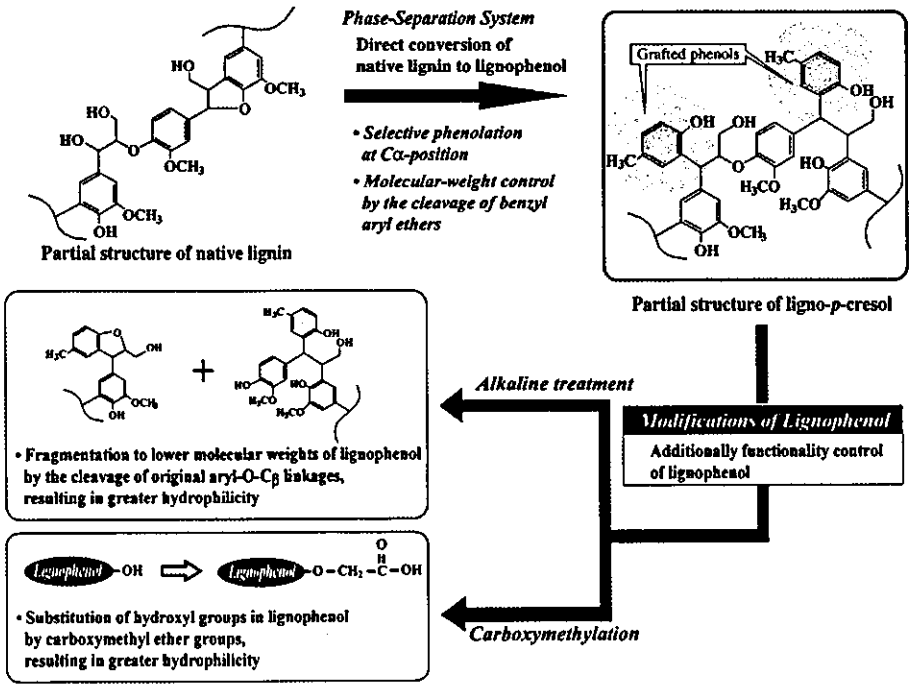

Figure 1. Conversion of native lignin into lignophenol derivatives and control of their functionality.

Table 1. Properties of lignophenol derivatives and the effect of various lignophenol derivatives on H_2O_2-induced apoptosis in SH-SY5Y cells

No.	Lignophenol derivatives	Properties of lignophenol derivatives				Antiapoptotic effect
		Hydroxyl groups** (mol/C_9)		Combined carboxymethyl groups***(mol/C_9)	Weight average molecular weight**** ($\overline{M}_W$)	
		Phenolic OH	Total OH			
1	Lignin alkali	—	—	—	28,000	+
2	Lignopyrogallol (Japanese cedar)	3.61	4.27	—	3410	–
3	Lignocatechol (Japanese cedar)	2.78	3.46	—	4820	–
4	Lignoresorcinol (Japanese cedar)	2.66	3.37	—	4810	+
5	Lignopyrogallol (rice husk)	Not measured		—	1950	–
6	AT-lignopyrogallol (Japanese cedar)	3.11	3.63	—	2430	–
7	CM-lignocresol (rice husk)	0.62	1.53	0.60	3810	+
8	CM-lignocresol (bamboo)	0.46	1.31	0.66	5330	+++
9	CM-lignocresol (beech)	0.64	1.75	0.67	5460	+
10	CM- and AT-lignocresol* (beech)	0.63	1.77	0.75	1500	+
11	AT-lignocresol (beech)	1.21	2.18	—	1700	++

(–) No effect, (+) blockage 0–25%, (++) 25–50%, (+++) 50–100%.

AT—alkaline-treated, CM—carboxymethylated.

All lignophenol derivatives are water-soluble. (*) Carboxymethylated materials of the water-insoluble fraction of alkaline-treated lignocresol. (**) Hydroxyl groups of lignopolyphenols and CM-derivatives were determined by ^{1}H NMR spectra for original lignopolyphenols in $CDCl_3$–$C5D_5N$ (1:3, v/v) and their acetylated derivatives in $CDCl_3$ (containing TMS as the internal reference) and nonaqueous potentiometric titration, respectively. (***) Carboxy methyl groups were determined by nonaqueous potentiometric titration. (****) Average molecular weights were calculated by gel permeation chromatograms (columns; Shodex KF602, KF603, and KF604, eluent; tetrahydrofuran, detector; UV at 280 nm) for acetylated derivatives, and which of lignin alkali was provided by technical data of Aldrich chemical company, Inc.

However, when water-insoluble lignophenols were carboxymethylated (CM) and/or alkaline-treated (AT), they became highly hydrophilic and water-soluble. Especially, CM-lignophenols showed a high binding affinity for proteins because of the introduced carboxyl groups.[5] The carboxymethyl groups were recognized by ^{1}H NMR (Table 1) and IR spectroscopy (Fig. 2). Signals at δ 4.6 in the NMR spectra of CM-lignophenols (lig-8), which were absent in the original lignophenols, were due to the methylene protons of the $-OCH_2COOH$ groups. As shown in Figure 2, absorption bands around 1600–1710 and 1425 cm^{-1} in the IR spectra of CM-lignocresols were markedly increased in intensity compared with those of original lignophenols after phase-separation, due to the overlapped absorptions of introduced carboxyl groups and aromatic nuclei in the original lignophenols (Fig. 2). The molecular weights of lignopolyphenols with or without AT and/or CM-lignophenols were within range of 1500–5500 or 2000–5000, respectively (Table 1).

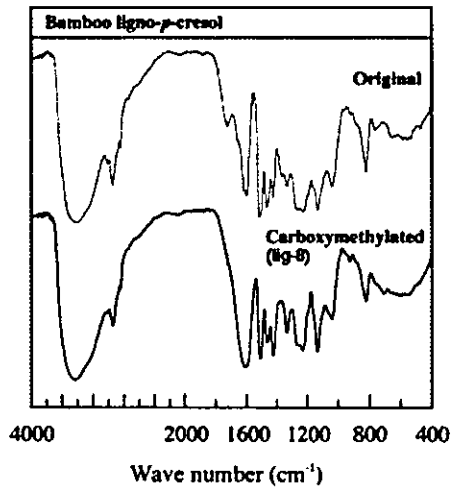

Figure 2. IR spectra of original (preparation after phase-separation) and carboxymethylated bamboo lignocresol derivative, lig-8.

2.2. Protective effects of lignophenol derivatives against the apoptosis induced by oxidative stress

We examined the ability of various lignophenol derivatives to protect SH-SY5Y cells from hydrogen peroxide (H_2O_2)-induced cell death. First, we determined the concentration of H_2O_2 required to induce apoptotic cell death by incubation for 12 h and the concentrations of 75–100 μM were found to be enough to induce apoptosis. The cell death induced by H_2O_2 at 100 μM for 12 h was found to be due to apoptosis, because the morphological findings characteristic of apoptosis such as nuclear condensation and fragmentation assessed by Hoechst 33342 nuclear staining, as well as DNA ladder formation were observed (Fig. 3). Next, we evaluated the apoptosis-blocking effect of various lignophenol derivatives (10–50 μM) for 12 h. To circumvent a direct effect of the compounds on externally added ROS in the medium, the compounds were added after the treatment with H_2O_2 for 2 h. As shown in Table 1, 7 of the 11 lignophenol derivatives tested exhibited the protective activity in the H_2O_2-induced apoptosis at 30 μM. The lignocresol derivatives were more potent in the neuroprotective activity compared with other lignophenols. Especially, the CM-lignocresol from bamboo named lig-8, displayed the most potent apoptosis-preventing activity at 20 and 30 μM. We used this compound for the following experiments for comparison with epigallocatechin gallate (EGCG) from green tea, which has been reported to protect against neuronal cell death induced by oxidative stress.[12,13,18] Lig-8 had no effect on the growth of SH-SY5Y cells at the concentrations of 10–50 μM, whereas EGCG showed cytotoxicity at more

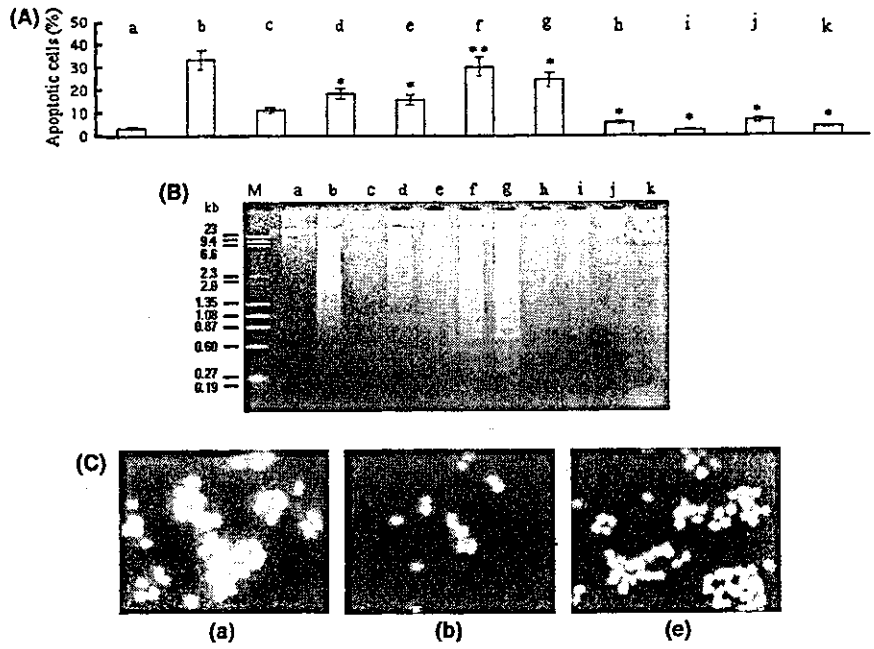

Figure 3. H_2O_2 or SIN-1-induced apoptosis and its blockage by the treatment with lig-8 or EGCG for 12h in SH-SY5Y cells. (A) Apoptotic cell death evaluated by Hoechst 33342 staining. Results are the mean ±SD of three independent experiments, $^{*}p<0.01$; $^{**}p<0.05$ versus b or c. (B) Apoptotic cell death evaluated by DNA ladder formation. (a) Control (untreated cells); (b) H_2O_2 100 μM; (c) SIN-1 500 μM; (d) H_2O_2 100 μM plus lig-8 20 μM; (e) H_2O_2 100 μM plus lig-8 30 μM; (f) H_2O_2 100 μM plus EGCG 10 μM; (g) H_2O_2 100 μM plus EGCG 20 μM; (h) SIN-1 500 μM plus lig-8 20 μM; (i) SIN-1 500 μM plus lig-8 30 μM; (j) SIN-1 500 μM plus EGCG 10 μM; (k) SIN-1 500 μM plus EGCG 20 μM. (C) Microscopic observation of cells treated with H_2O_2 alone (b) or H_2O_2 plus lig-8 (e) in Hoechst 33342 nuclear staining. Untreated control cells (a).

than 30 μM (data not shown). Lig-8 significantly prevented H_2O_2-induced apoptosis at 20 or 30 μM, whereas EGCG at 10 or 20 μM exhibited a marginal antiapoptotic effect (Fig. 3A and B). In the case of apoptosis induced by 3-(4-morpholinyl)sydonimine (SIN-1)[20] which generates RNS in cells,[21] lig-8 also exerted a potent protection against apoptosis at the same concentrations as in the H_2O_2-induced apoptosis. EGCG was more protective against SIN-1-induced apoptosis than H_2O_2-induced one (Fig. 3A and B).

In order to determine the site(s) of lig-8's action in the signaling pathway of apoptosis, we examined the activation of an apoptosis executioner caspase, caspase-3, by Western blot analysis. The 18-kD active form of caspase-3 was discernible at 6h after the treatment with 100 μM H_2O_2 (Fig. 4A). However, such active form was not detected in the paired sample from the cells treated with 100 μM H_2O_2 in the presence of lig-8, suggesting that lig-8 blocked the caspase-3 activation. In order to further confirm the involvement of caspase-3 activation in apoptosis, we examined the effects of a caspase-3 inhibitor Z-DEVD-FMK and a pan-caspase inhibitor Z-VAD-FMK on apoptosis. It was shown that the inhibitors efficiently prevented the apoptosis in a concentration-dependent manner, as judged by Hoechst 33342 nuclear staining (Fig. 4B). The inhibitor almost blocked the apoptosis at 100 μM. In addition, the activation of apoptosis initiator caspase-8 was clearly demonstrated by colorimetric protease assay (Fig. 5A) and dose-dependent apoptosis inhibition was shown by assay using a caspase-8 inhibitor Z-IETD-FMK (Fig. 5B). Thus, H_2O_2-induced apoptosis in SH-SY5Y cells

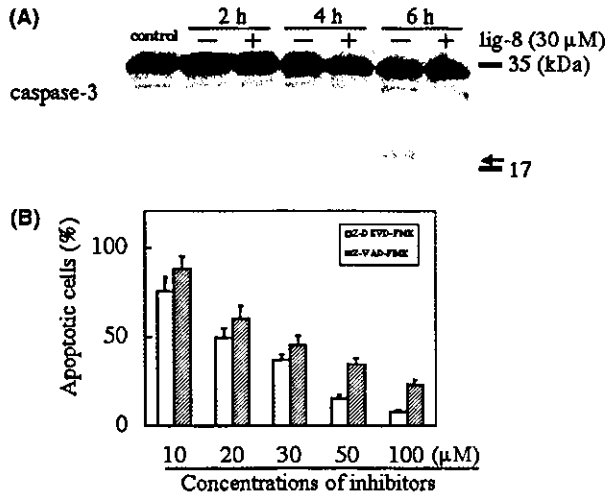

Figure 4. Involvement of caspase-3 activation in the H_2O_2-induced apoptosis and inhibition of caspase-3 activation by lig-8. (A) Western blot analysis of caspase-3. The arrow indicates the active form of caspase-3. (B) Apoptosis inhibition assay using caspase-3 inhibitor Z-DEVD-FMK or pan-caspase inhibitor Z-VAD-FMK. The apoptotic cell death was evaluated by Hoechst 33342 staining. Results are the mean±SD of three independent experiments. The percentage of apoptotic cells without the inhibitor is as 100%.

was exerted through the activation of both caspase-8 and -3. However, lig-8 did not affect the activation of caspase-8 (Fig. 5A).

In the apoptosis inhibition assay using pan-caspase or caspase-3 inhibitor, addition of lig-8 reduced the dose

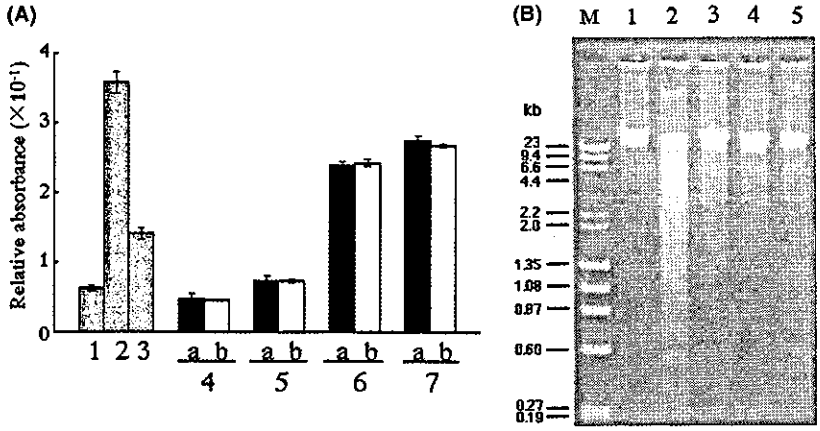

Figure 5. Involvement of caspase-8 in the H_2O_2-induced apoptosis examined by colorimetric protease assay and apoptosis inhibition assay using Z-IETD-FMK in SH-SY5Y cells. (A) Colorimetric protease assay of caspase-8 in H_2O_2-induced apoptosis. Each sample was prepared described in Experimental. Column 1, Jurkat cells without treatment; 2, Jurkat cells treated with ant-Fas antibody for 3 h; 3, Jurkat cells treated with ant-Fas antibody in the presence of caspase-8 inhibitor (Z-IETD-FMK); (columns 4–7: (a) treatment with 100 μM H_2O_2, (b) treatment with 100 μM H_2O_2 plus 30 μM lig-8); 4, SH-SY5Y cells before treatment; 5, treated for 2 h; 6, treated for 4 h; 7, treated for 6 h. The values of absorbance at 405 nm are expressed. Means ±SD of three independent experiments are given. (B) Activation of caspase-8 in SH-SY5Y cells examined by apoptosis inhibition assay. Three micrograms of DNA was applied onto each lane. The inhibitor for caspase-8, Z-IETD-FMK, was added 6 h before exposure to 100 μM H_2O_2. The rescue of cell death was evaluated at 12 h after 100 μM H_2O_2 exposure by reduced formation of nucleosomal DNA fragments at each concentration of the inhibitor. Lane 1, DNA from cells in the presence of 0.01% DMSO and 60 μM Z-IETD-FMK (control); lane 2, treatment with 100 μM H_2O_2 for 12 h; lane 3, with 100 μM H_2O_2 plus 20 μM inhibitor; lane 4, with 40 μM inhibitor; lane 5, with 60 μM inhibitor. Lane M is a DNA size marker.

of Z-DEVD-FMK or Z-VAD-FMK to exert the equivalent antiapoptotic efficacy (data not shown). These results led us to explore the in vitro effect of lig-8 in the process of procaspase-3 proteolysis. Lig-8 was added to the reaction mixture containing SH-SY5Y cell lysate and the recombinant active caspase-8 in tubes, and its effect on caspase-3 activation was examined by Western blot analysis. Lig-8 dose-dependently prevented the proteolysis of procaspase-3 by recombinant active caspase-8 (Fig. 6A). Indeed, the higher concentrations of lig-8 were needed to suppress the activation of caspase-8, but the results from in vivo and in vitro experiments suggested that lig-8 possibly blocked the activation of caspase-3.

In the last several years, it has become increasingly clear that mitochondria play a major rate-limiting role in the apoptosis of neuronal cells. The decision/effector phase of the apoptotic process converges on mitochondria, where permeabilization of mitochondrial membranes occurs as a result of the permeability transition pore complex (PTPC).[22,23] We next examined the effect of lig-8 on mitochondrial membrane PT in the apoptosis. The mitochondrial membrane potential examined by FACS clearly showed a decrease in the cells treated with H_2O_2 for 8 h and its decrease was significantly reduced in the presence of lig-8 (Fig. 7A). Furthermore, the release of cytochrome c from mitochondria and simultaneously the sequential activation of caspase-9 were also

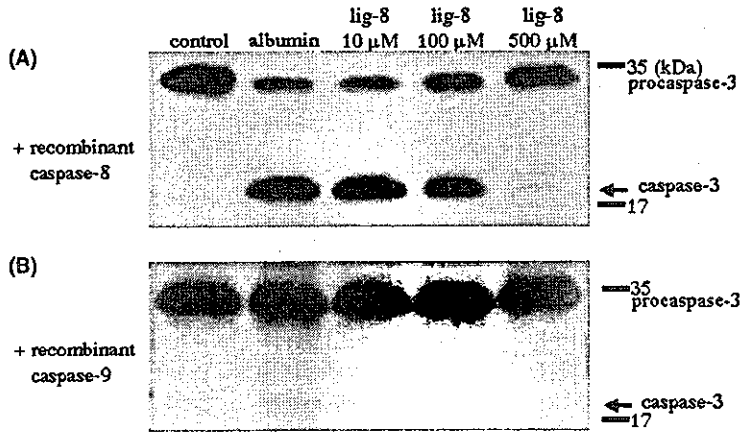

Figure 6. Effect of lig-8 on proteolytic cleavage of procaspase-3 by recombinant caspase-8 or caspase-9 in vitro examined by Western blot analysis. (A) Proteolysis of procaspase-3 by recombinant caspase-8. (B) The proteolysis of procaspase-3 by recombinant caspase-9. The cell lysate without recombinant caspase-8 is used as a negative control. We added albumin to reaction buffer as a positive control.

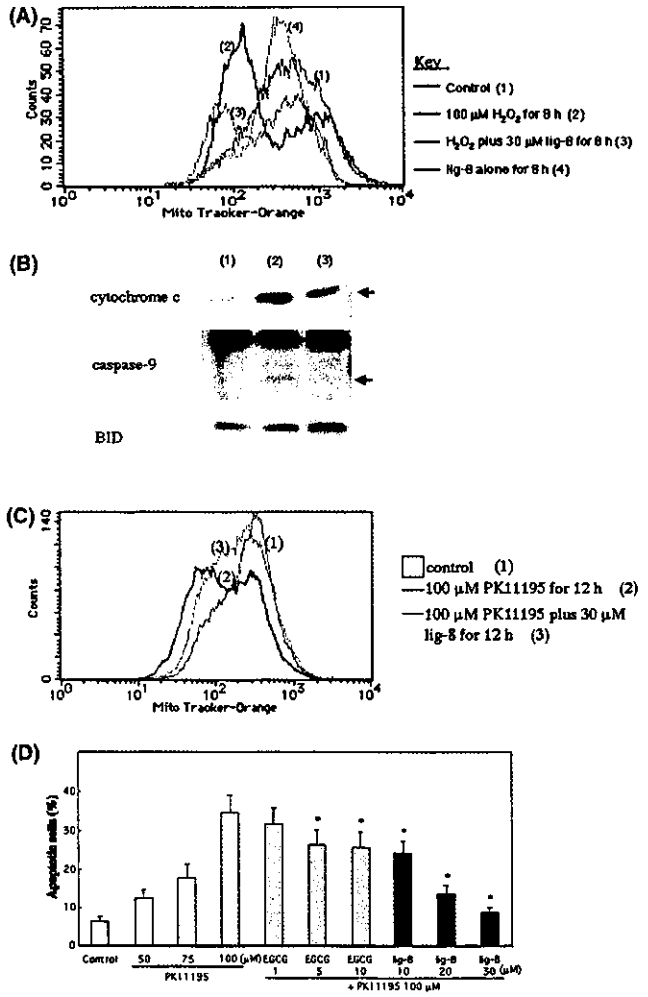

Figure 7. Effect of lig-8 on mitochondrial membrane potential and release of cytochrome c in the H_2O_2- or PK11195-induced apoptosis. (A) Mitochondrial membrane potential examined by FACS using Mito–Tracker Orange or Green. The cells were treated for 8 h with 100 μM H_2O_2 (trace 2), 100 μM H_2O_2 plus 30 μM lig-8 (trace 3), or lig-8 alone (trace 4). Control (trace 1) is untreated cells. The patterns of fluorescence intensity of Mito–Tracker Green were almost similar in the samples tested. (B) Western blot analysis of cytochrome c, caspase-9, and BID at 8 h after the treatment with 100 μM H_2O_2 (lane 2) or 100 μM H_2O_2 plus 30 μM lig-8 (lane 3). Lane 1 is untreated cells (control). The lane numbers correspond to the same numbers in (A). (C) Mitochondrial membrane potential in PK11195-induced apoptosis examined by FACS using Mito–Tracker Orange or Green. The cells were treated for 12 h with 100 μM PK11195 (trace 2) or 100 μM PK11195 plus 30 μM lig-8 (trace 3). Control (trace 1) is untreated cells. The patterns of fluorescence intensity of Mito–Tracker Green were almost similar in the samples tested. (D) Comparison of the apoptosis-inhibitory activity between lig-8 and EGCG in PK11195-induced apoptosis evaluated by Hoechst 33342 nuclear staining. Results are the mean ± SD of three independent experiments, $^*p<0.01$ versus the value of apoptotic cells (%) in 100 μM PK11195 treatment.

suppressed by lig-8 (Fig. 7B). Thus, H_2O_2-induced apoptosis is considered to be mediated via the mitochondrial pathway, and lig-8 was shown to ameliorate the apoptosis by preventing depolarization of mitochondrial membrane PT. The truncated BID, which induces the release of cytochrome c from mitochondria without mitochondria potential loss,[23] was not observed by Western blot analysis (Fig. 7B). Considering the time course of the apoptosis, the activation of caspase-8/3 likely affects the mitochondrial pathway.

In order to further assess the effect of lig-8 on mitochondrial membrane PT, we examined the changes in mitochondrial membrane potential induced by a peripheral benzodiazepine receptor (PBR) ligand, 1-(2-chlorophenyl)-N-(1-methylpropyl)-3-isoquinolinecarboxamide (PK11195).[24,25] FACS demonstrated that the decrease in mitochondrial membrane potential by 100 μM PK11195 was considerably prevented by lig-8 at 30 μM (Fig. 7C). Moreover, the activation of caspase-9 by PK11195 was almost blocked by 30 μM lig-8 (data not shown) and therefore, lig-8 significantly inhibited the apoptosis in a concentration-dependent manner, whereas EGCG only slightly inhibited the PK11195-induced apoptosis (Fig. 7D). Thus, lig-8 was able to prevent PK11195-induced cell death mediated by mitochondrial membrane PT, as observed in H_2O_2-induced cell death. Based on these data, we also examined the effect of lig-8 on in vitro proteolysis of the recombinant active caspase-9, and showed that lig-8 prevented proteolysis of procaspase-3 (Fig. 6B). Taken together, these data suggest that the antiapoptotic effect of lig-8 was most likely due to its action on the caspase-3 proteolytic process by caspase-8 and -9, and also on depolarization of mitochondrial membrane PT.

The level of intracellular ROS measured by FACS using CM-H_2 DCF-DA at 2 h after the treatment with H_2O_2 was slightly increased. However, the level in H_2O_2/lig-8- and H_2O_2/EGCG-cotreated cells was reduced, indicating that lig-8 as well as EGCG exerted an ROS-scavenging effect (Fig. 8A, right panel). Even though the level of intracellular ROS at 30 min after the treatment compensatively decreased in the H_2O_2-treated cells (Fig. 8A, left panel), the ROS scavenging activity of lig-8 was also observed. Perhaps the ROS scavenging activity of lig-8 is more potent than that of EGCG. These results were consistent with those in in vitro ROS-scavenging test (Fig. 8B, left panel). EGCG may scavenge more NO radicals compared with lig-8 in in vitro ROS-scavenging test (Fig. 8B, right panel), which possibly reflected the results of cell death assay in Figure 3A.

The results in the present study have provided the first demonstration that lignophenol derivatives protected human dopaminergic neuroblastoma SH-SY5Y cells against cell death due to apoptosis induced by oxidative stress. We were successful in converting the native lignins to bioactive lignophenols, which have almost original 3-dimentional network structures by using the phase-separation technique. Among various lignophenols, lignocresol derivatives exhibited higher apoptosis-blocking activity than other lignophenols tested. Lig-8, the water-soluble carboxymethylated (CM)-lignocresol from bamboo, displayed the most potent preventive effect on the apoptosis induced by oxidative stress such as H_2O_2 and NO in SH-SY5Y cells.

Native lignin has various complex structures with inter-unit linkages, polyphenolic groups, and a 3-dimensional branched network. Furthermore, the chemical proper-

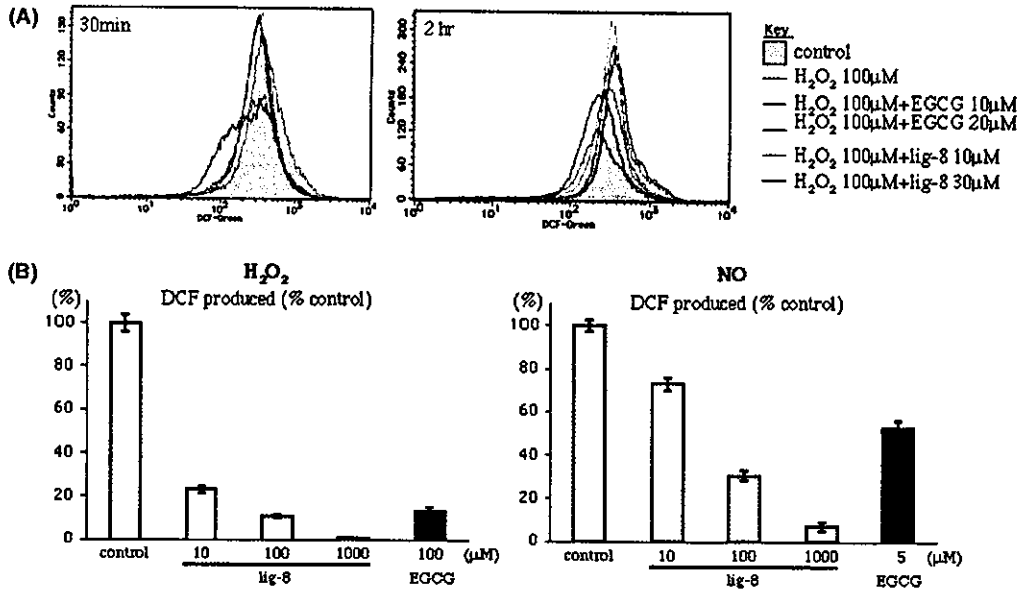

Figure 8. Antioxidant activity of lig-8. (A) The intracellular ROS levels scavenged by EGCG or lig-8 after H_2O_2-treatment in SH-SY5Y cells was measured by FACS as described in Experimental. The cells in the medium without FCS were treated with 100 μM H_2O_2 for 30 min or 2 h. (B) The levels of ROS generated from H_2O_2 or a nitric oxide donor, Nor-4, were quantified by measuring the fluorescence intensity of DCF, and the scavenging potencies of EGCG and lig-8 were expressed as the percentage of control without the antioxidants. The average of two independent measurements is given.

ties of lignins, especially the network structures, differ greatly depending on the lignocellulosics, because the precursors bulging up lignin differ in their species. Generally, softwood lignins consist mainly of guaiacyl aromatic units, and hardwood lignins contain evenly guaiacyl and syringyl units. On the other hand, herb lignins including bamboo have parahydroxy phenyl units rather than these units. Certainly, the structure containing the parahydroxy phenyl units in bamboo lignin and the additional phenolic groups may contribute to the neuroprotective activity of lig-8. However, further studies of the structure–activity association are necessary to determine the units or groups involved in the activity.

The apoptosis induced by H_2O_2 in SH-SY5Y cells was mediated by activation of caspase-3, which was confirmed by Western blot analysis and the apoptosis inhibition assay using the caspase-3 inhibitor Z-DEVD-FMK or pan-caspase inhibitor Z-VAD-FMK. Lig-8 significantly prevented activation of caspse-3 at 6 h after the treatment with H_2O_2. The apoptosis was completely blocked by the incubation with either 100 μM Z-VAD-FMK or Z-DEVD-FMK. Addition of various concentrations of lig-8 to the inhibitor clearly reduced amount of the inhibitors in dose-dependent manner to compensate the apoptosis-blocking ability in 100 μM of the inhibitor (data not shown). These results raise the possibility that lig-8 may directly block the activation of caspase-3 and/or other caspases. Then, we examined the activation of caspase-8, as an initiator caspase of apoptosis, which acts upstream of procaspase-3. By colorimetric protease assay using substrate of caspase-8, we found that the activation of caspase-8 is involved in the apoptosis. However, we could not obtain the positive data that lig-8 affects the activation. In the light of these data, we examined the proteolysis blocking effect of lig-8 on caspase-3 activation in vitro and found that lig-8 blocked the proteolysis of procaspase-3 by recombinant active caspase-8 in a dose-dependent manner. However, the higher concentrations of lig-8 were needed to see inhibition in caspase-3 activation, compared with those of in vivo. Therefore, although it can be considered that lig-8 rescues cells from the apoptosis by inhibiting the activation of caspase-3 via caspase-8, antiapoptotic effect of lig-8 is at least in part mediated through caspase-8/3. Similarly, the in vitro proteolysis inhibition assay using the recombinant active caspase-9 showed the ability of lig-8 to inhibit the proteolytic cleavage of procaspase-3. To define the specificity of lig-8's action to inhibit procaspase-3 proteolysis via caspase-8 or -9, further experiments are required.

It has been earlier reported that the caspase-8 activation is mediated by induction of Fas expression in H_2O_2-induced apoptosis in B-cell lymphoma cells.[26] However, we did not obtain any evidence causing caspase-8 activation in the H_2O_2-induced apoptosis.

On the other hand, lig-8 significantly prevented the depolarization of mitochondrial membrane potential at 8 h after the treatment, as judged by FACS analysis using Mito-Tracker fluorescent probes. Moreover, Western blot analysis of cytochrome c indicated marked suppression of cytochrome c release from mitochondria by lig-8. In order to further confirm lig-8's action on mitochondrial membrane PT, we examined the effect of lig-8 in PK1195-induced apoptosis involving the loss of mitochondrial membrane PT.[24,25] As observed in H_2O_2-induced apoptosis, lig-8 considerably protected the cells from PK11195-induced apoptosis by preventing the loss of PT. Lig-8 may affect the interaction of PK11195 with peripheral benzodiazepine receptor

(PBR), in part, by competitive inhibition. In Bcl-2-over-expressing SH-SY5Y cells, PK11195-induced apoptosis was completely blocked (data not shown). Therefore, its mode of prevention of apoptosis was different from that by lig-8, suggesting that the PBR receptor on the mitochondrial membrane may be closely associated with molecules of PTPC including Bcl-2/Bax and VDAC.[27] Thus, lig-8 prevents the depolarization of mitochondrial membrane PT in both cases. Since the caspases-8/3 pathway (6 h after H_2O_2-treatment) precedes the mitochondrial pathway (8 h after H_2O_2-treatment), it is suggested that the activation of caspase-8/3 may affect the mitochondrial pathway via caspase-2.[28,29] In fact, the caspase-2 inhibitor Z-VDVAD-FMK significantly blocked the apoptosis dose-dependently, however, lig-8 did not affect the activation of caspase-2 (data not shown) and the truncated BID acting on mitochondria was not observed.

As for the antioxidant activity of lig-8, we have demonstrated that the intracellular ROS level of H_2O_2-treated cells was decreased by addition of lig-8. Its scavenging activity was also shown in in vitro ROS-scavenging test and even on superoxide (data not shown). Therefore, lig-8 likely exerts its protective activity by scavenging ROS. In comparison with EGCG, which has been reported to exert neuroprotective effect because of its antioxidant activity,[12,13,18] lig-8 attenuated the cell death induced by either H_2O_2 or nitric oxide free radical donor SIN-1 in SH-SY5Y cells. In addition, our data suggest that EGCG may scavenge RNS produced by NO generating agent SIN-1-rather than ROS by H_2O_2-treatment. Since the preventive effect of lig-8 is mainly due to blockage of the apoptotic signaling pathway, the mechanism(s) underlying preventive effect for cell death by lig-8 seems likely to be different from that by EGCG.

Recently, some phytochemicals are considered to be beneficial for prevention of neuronal cell death by affecting the intracellular signal transduction pathway. EGCG has protective effects against Aβ-induced apoptosis through regulation of the secretory process of non-amyloidogenic amyloid precursor protein via protein kinase C (PKC).[30] Quercetin prevents the H_2O_2-mediated mitochondrial dysfunction by preserving mitochondrial membrane PT as well as an increased in expression of BCL-2 and BCL-X(L) in cardiomyoblast cells.[31] It was also reported that quercetin exhibits a protective action against NO-induced toxicity via PKC pathway in cultured rat hippocampal cells.[32] In our cases, the levels of phosphorylated ERK and p38 were changed, but they were not affected by lig-8.

Lig-8 also exhibited an antiapoptotic activity against H_2O_2-induced apoptosis even in rat neuroblastoma cell line PC12. More extensive studies are necessary for elucidation of the apoptosis-inhibitory activity of lig-8 in primary cultured neuronal cells and in animal models, which are under current progress in our laboratory. Lig-8 is considered to exhibit a more potent neuroprotective effect compared with EGCG because of the direct action on apoptosis signal pathways. The results of our current study suggest that lignocresol derivatives would be a candidate for agent to rescue the neuronal cells from cell death induced by the oxidative stress that accelerates the progression of neurodegenerative diseases.

3. Conclusion

In the present work it was demonstrated that by using our newly developed phase-separation technique lignin, a durable aromatic network polymer second to cellulose in abundance was able to be converted into highly active lignophenol derivatives with antioxidant activity. These lignophenol derivatives were found to show the potent neuroprotective activity against oxidative stress. Among the compounds examined, a lignocresol derivative from bamboo (lig-8) exhibited the most potent neuroprotective activity against hydrogen peroxide (H_2O_2)-induced apoptosis in human neuroblastoma cell line SH-SY5Y by preventing the caspase-3 activation via either caspase-8 or caspase-9. Furthermore, it was found that lig-8 exerted the antiapoptotic effect by inhibiting dissipation of the mitochondrial membrane permeability transition induced by H_2O_2 or by the peripheral benzodiazepin receptor ligand PK11195. These data suggest that lig-8 is a promising neuroprotector, which affects the signaling pathway of neuronal cell death and that it would be of benefit to delay the progress of neurodegenerative diseases.

4. Experimental

4.1. Lignocellulosics and lignin preparation

Air-dried lignocellulosics (softwood, Japanese cedar [*Cryptomeria japonica*]; hardwood, Japanese beech [*Fagus crenata*]; herbs, rice husk [*Oryza sativa*], and bamboo [*Phyllostachys bambusoides*]) were milled until they could pass through a 100 μm screen and then extracted with ethanol–benzene (1:2, v/v) for 48 h. Extracts of these lignocellulosics were air-dried to remove the solvent and then the extract were treated with pepsin solution by Ellis's method[33] to prepare their protein-free form. Lignin alkali (Aldrich Chemical Co. Inc., WI) was used as conventional lignin, kraft lignin.

4.2. Synthesis and isolation of lignophenol

Using a modified phase-separation system (Two-step process I) (Fig. 1),[2] we synthesized water-insoluble ligno-*p*-cresol and water-soluble ligno-catechol, -resorcinol, and -pyrogallol. These phenols (monohydric phenol *p*-cresol and polyhydric phenols catechol, resorcinol, and pyrogallol; 3 mol/C9 [C9 is lignin building unit]) were sorbed to extract solvent-free wood or protein-free herb meals. Sulfuric acid (72%, 20 mL/g lignocellulosics) was added to the lignocellulosics-sorbed phenols, and the mixture was vigorously stirred at room temperature for 1 h. Phenol–benzene solution (7:3, v/v) was added to the mixture with stirring. After stirring, the reaction mixture was separated into two phases, organic and aqueous phases. The organic phase was taken up and then an excess amount of ethyl ether was added drop-

wise with vigorous stirring. The resultant precipitates were dissolved in acetone and the insoluble substance was removed. The aqueous phase was mixed with excess water and centrifuged. The supernatant was neutralized with NaOH, dialyzed, and freeze-dried. The dried material was extracted with methanol, and then the soluble fraction was added dropwise to an excess amount of ethyl ether with stirring. The precipitate (water-soluble lignophenol) was collected by centrifugation and dried over P_2O_5 after evaporating the solvent.

4.3. Selective cleavage of lignophenols by alkaline treatment

The aryl ether linkages of lignophenols were selectively cleaved by alkaline treatment.[2] For this, water-insoluble ligno-*p*-cresol from the organic phase was treated with 0.5N NaOH (20mL/g lignophenol) at 170°C for 1h and the reaction mixture was then acidified to pH2 with 1N HCl and centrifuged. The resultant precipitate (water-insoluble fraction) was collected by centrifugation, washed several times, and dried over P_2O_5. The supernatant (water-soluble fraction) was dialyzed and freeze-dried.

4.4. Carboxymethylation of lignophenol

Water-insoluble lignocresol from the organic phase or water-insoluble fraction of alkaline-treated lignocresol was dissolved in isopropanol (IPA, 4g/g lignophenol), and 40 % NaOH (2.5g/g lignophenol) was added with stirring. Then, monochloroacetic acid (1.6mol/mol hydroxyl group in lignophenol) in isopropanol (4g/g lignophenol) was added and stirred further at 50°C for 2h. The resultant precipitate including carboxymethylated (CM-) lignophenols was collected by centrifugation, dissolved in water, and acidified to pH2. The insoluble fraction was removed by centrifugation and the supernatant containing the water-soluble CM-lignophenols was dialyzed and then freeze dried.

4.5. Structural analysis of lignophenols

The amounts of combined phenols and hydroxyl groups in the lignophenols were calculated from ^{1}H NMR spectra of acetylated lignophenols obtained with a JEOL JNM-LA300 FT-NMR. *p*-Nitrobenzaldehyde was used as the internal reference for their determination. The extents of the carboxymethylation were estimated by infrared (IR) spectroscopy (KBr disks, JASCO FT/IR-8900m) and NMR spectroscopy. The average molecular weights were measured by gel permeation chromatography on a JASCO GULLIVER 1500 system, PU-1585, UV-1570 with two columns (Shodex OH-pak SB-803 HQ, SB-806M HQ). Sodium chloride (10μM) was used as the eluent.

4.6. Cell culture and treatment of SH-SY5Y

Human neuroblastoma cell line SH-SY5Y was cultured in MEM supplemented with 5% fetal calf serum (FCS) and maintained at a density of 2×10^5 cells per mL before treatment. For the experiments, the cells were seeded at the density of $1–2\times10^5$/mL in 60mm diameter wells and cultured for 12h. After the cells were pretreated with hydrogen peroxide (H_2O_2; Wako, Tokyo), 3-(4-morpholinyl)sydonimine (SIN-1; Dojindo, Kumamoto, Japan), and 1-(2-chlorophenyl)-N-(1-methylpropyl)-3-isoquinolinecarboxamide (PK11195; TOCRIS, MO) for 2h, agents such as lignophenol derivatives and epigallocatechin gallate (EGCG; Wako) were added to the cell cultures at selected concentrations.

4.7. Assessment of apoptosis

For assessment of the morphological characteristics of apoptosis, the cells were stained with Hoechst 33342 (5μg/mL) at 37°C for 30min, washed once with PBS, resuspended and pipetted dropwise onto a glass slide, and examined by fluorescence microscopy using an Olympus microscope (Tokyo, Japan) equipped with an epi-illuminator and appropriate filters. The cells with condensed and fragmented nuclei stained with Hoechst 33342 were assessed to be apoptotic. In all conditions examined, necrotic cell death by H_2O_2 was negligible (less than 2% of the total cells). Approximately 200 cells were counted in four different fields and three independent experiments were performed. To examine nucleosomal DNA fragmentation by agarose gel electrophoresis, cellular DNA was extracted from whole cells by ethanol precipitation after phenol/chloroform preparation. RNase was added to the DNA solution at the final concentration of 20μg/mL, and the mixture was incubated at 37°C for 30min. After electrophoresis on a 2.5% agarose gel, DNA was visualized by ethidium bromide staining. For the apoptosis inhibition assay, a caspase-3 inhibitor, Z-DEVD-FMK (MBL, Nagoya, Japan), a pan-caspase inhibitor, Z-VAD-FMK (MBL), a caspase-8 inhibitor, Z-IETD-FMK (MBL), or a caspase-2 inhibitor, Z-VDVAD-FMK (Sigma, Saint Louis, MO) was added at the desired concentrations to the medium 30min before the H_2O_2 treatment.

4.8. Western blot analysis

SH-SY5Y cells were washed twice with PBS, suspended in lysis buffer A or B and then homogenized. Lysis buffer A (2×PBS, 0.1% SDS, 1% Nonidet P-40, 0.5% sodium deoxycholate, and 25×complete, protease inhibitor (Roche, Penzberg Germany)) was used to analyze caspases and BID. Lysis buffer B (250mM sucrose, 20mM Hepes-KOH (pH7.5), 10mM KCl, 1.5mM $MgCl_2$, 1mM EDTA, 1mM EGTA, 1mM DTT, and 25×Complete) was used to analyze AIF and cytochrome c. The mitochondrial and cytosolic fractions were prepared by the centrifugation after the incubation with Lysis buffer B. Five micrograms of lysate protein was separated by SDS-PAGE using a 12% polyacrylamide gel and electroblotted onto a PVDF membrane (Du Pont, Boston, MA). After blockage of nonspecific binding sites for 1h with 5% nonfat milk in PBS containing 0.1% Tween 20, the membrane was incubated overnight at 4°C with antihuman caspase-3 (Transduction Laboratories, Lexington, KY), antihuman caspase-9 (MBL), antihuman cytochrome c (R&D Systems, Minneapolis,

MN), or antihuman BID (R&D Systems) antibody. The membranes were then washed three times with PBS containing 0.1% Tween 20, incubated further with alkaline phosphatase-conjugated goat antimouse antibody (Promega, Madison, WI) at room temperature, and then washed three times with PBS containing 0.1% Tween 20. The immunoblots were visualized by use of an enhanced chemiluminescence detection kit (New England Biolabs, Beverly, MA).

4.9. In vitro proteolysis of procaspase-3 by caspase-8 or -9

Protein (1 μg) of SH-SY5Y cell lysate was incubated at 37 °C for 1 h with 1 unit or 3 units of recombinant caspase-8 (MBL) or −9 (MBL), respectively, in the solution containing 50 mM Hepes (pH 7.2), 50 mM NaCl, 0.1% Chaps, 10 mM EDTA, 5% glycerol, and 10 mM DTT. The proteolytic cleavage was assessed by Western blot analysis.

4.10. Measurement of mitochondrial membrane potential

Mitochondrial membrane potential was measured by use of the fluorescent dyes, Mito–Tracker Green (Molecular Probes, #M-7514, Eugene, OR) estimating the mitochondrial volume, and Mito–Tracker Orange (Molecular Probes, #M-7511), which accumulates selectively in active mitochondria. After the cells were washed twice with RPMI-1640 medium, the treated or untreated cells were incubated with Mito–Tracker fluorescent probes (100 nM each) for 30 min at 37 °C. Then the cells were collected, washed twice with PBS, and resuspended in PBS. The fluorescence of Mito–Tracker Orange and Green was analyzed by fluorescence activated cell sorter (FACS; Becton Dickinson, San Jose, CA).

4.11. Measurements of production and scavenging activity of reactive oxygen or reactive nitrogen species

The production of reactive oxygen species (ROS) was monitored by the use of 5-(and-6)-chloromethyl-2′,7′-dichlorodihydrofluorescein diacetate (CM-H_2 DCF-DA; Molecular Probes, Irvine, CA) or 2′,7′-dichlorodihydrofluorescein diacetate (H_2 DCF-DA; Molecular Probes). After the cells treated with or without H_2O_2 were washed twice with PBS, CM-H_2 DCF-DA (10 μM) was added to the cell suspension in PBS at 37 °C. After 30 min-incubation, the 2′,7′-dichlorodihydrofluorescein (DCF) in cells was determined by the FACS. The fluorometric measurement was performed with excitation and emission wavelengths of 495 and 530 nm, respectively. For the measurement of the in vitro ROS scavenging potency, ROS was produced in a 96-well microplate by incubation of 1 mM H_2O_2 or 1 mM nitric oxide donor, Nor-4 (Dojindo) in PBS at 37 °C and the effects of lig-8 or EGCG were examined by addition of their various concentrations. The increase of a fluorescent product, DCF from H_2 DCF-DA was followed in a MTP-600F (CORONA electronic, Hitachinaka, Japan) reader with excitation at 495 and 530 nm emission.

4.12. Colorimetric protease assay

The activation of caspase-8 was determined by colorimetric protease assay. Briefly, the cells treated with H_2O_2 were harvested at the indicated times, suspended in cell lysis buffer, and then incubated on ice for 10 min. The lysate containing 150 μg protein was incubated with 200 μM IETD-pNA substrate (MBL) at 37 °C for 2 h. Levels of released pNA were measured with a Nalgenunc spectrofluorometer at 405 nm. The cell lysate of Jurkat cells treated with anti-Fas antibody (clone CH-11) (MBL) for 3 h was used as a positive control for caspase-8 activation.

4.13. Statistical analysis

For the statistical analyses, 1-way ANOVA and Fisher's PLSD test were performed by using StatView software (SAS Institute Inc., Cary, NC).

Acknowledgements

We thank Ms. Nishizawa for her skillful assistance for these experiments. This work was supported by a grant from Medical Frontier Strategy Research (W.M., Y.A., and M.N.) from the Ministry of Health, Labor and Welfare, Japan.

References and notes

1. Funaoka, M.; Abe, I. *Tappi J.* **1989**, *72*, 145.
2. Funaoka, M.; Fukatsu, S. *Holzforschung* **1996**, *50*, 245.
3. Funaoka, M.; Matsubara, M.; Seki, N.; Fukatsu, S. *Biotechnol. Bioeng.* **1995**, *46*, 545.
4. Funaoka, M.; Ioka, H.; Hosho, T.; Tanaka, Y. *J. Network Polym.* **1996**, *17*, 121.
5. Suzuki, H.; Tochikura, T. S.; Iiyama, K.; Yamazaki, S.; Yamamoto, N.; Toda, S. *Agric. Biol. Chem.* **1989**, *53*, 3369–3372.
6. Ichimura, T.; Watanabe, O.; Maruyama, S. *Biosci. Biotechnol. Biochem.* **1998**, *62*, 575.
7. Jiang, Y.; Satoh, K.; Aratsu, C.; Kobayashi, N.; Unten, S.; Kakuta, H.; Kikuchi, H.; Nishikawa, H.; Ochiai, K.; Sakagami, H. *Anticancer Res.* **2001**, *21*, 965.
8. Thompson, C. B. *Science* **1995**, *267*, 1456.
9. Tatton, W. G.; Chalmes-Redman, R. M. E. *Ann. Neurol.* **1998**, *44*(Suppl 1), S134.
10. Kidd, P. M. *Altern. Med. Rev.* **2000**, *5*, 502.
11. Conrad, C. C.; Marshall, P. L.; Talent, J. M.; Malakowsky, C. A.; Choi, I.; Gracy, R. W. *Biochem. Biophys. Res. Commun.* **2000**, *275*, 678.
12. Lee, S. R.; Im, K. J.; Suh, S. I.; Jung, J. G. *Phytother. Res.* **2003**, *17*, 206.
13. Nagai, K.; Jiang, M. H.; Hada, J.; Nagata, T.; Yajima, Y.; Yamamoto, S.; Nishizaki, T. *Brain Res.* **2002**, *956*, 319.
14. Dona, M.; Dell'Aica, I.; Calabrese, F.; Benelli, R.; Morini, M.; Albini, A.; Garbisa, S. *J. Immunol.* **2003**, *170*, 4335.
15. Singh, R.; Ahmed, S.; Malemud, C. J.; Goldberg, V. M.; Haqqi, T. M. *J. Orthop. Res.* **2003**, *21*, 102.
16. Jung, Y. D.; Kim, M. S.; Shin, B. A.; Chay, K. O.; Ahn, B. W.; Liu, W.; Bucana, C. D.; Gallick, G. E.; Ellis, L. M. *Br. J. Cancer* **2001**, *84*, 844.
17. Sachinidis, A.; Seul, C.; Seewald, S.; Ahn, H.; Ko, Y.; Vetter, H. *FEBS Lett.* **2000**, *471*, 51.

18. Mira, L.; Fernandez, M. T.; Santos, M.; Rocha, R.; Florencio, M. H.; Jennings, K. R. *Free Radical Res.* **2002**, *36*, 1199.
19. Nanami, O.; Watanabe, Y.; Syuto, B.; Nakano, M.; Tsuji, M.; Kuwabara, M. *Free Radical Res.* **1998**, *29*, 359.
20. Oh-hashi, K.; Maruyama, W.; Yi, H.; Takahashi, T.; Naoi, M.; Isobe, K. *Biochem. Biophys. Res. Commun.* **1999**, *263*, 504.
21. Feelisch, M.; Ostrowski, J.; Noack, E. *J. Cardiovasc. Pharmacol.* **1989**, *14*, S13.
22. Zoratti, M.; Szabo, I. *Biochem. Biophys. Acta* **1995**, *1241*, 139.
23. Tsujimoto, Y.; Shimizu, S. *FEBS Lett.* **2000**, *466*, 6.
24. Vrabec, J. P.; Lieven, C. J.; Levin, L. A. *Invest. Ophth. Vis. Sci.* **2003**, *44*, 2774.
25. Solary, E.; Bettaieb, A.; Dubrez-Daloz, L.; Corcos, L. *Leukemia. Lymphoma* **2003**, *44*, 563.
26. Devadas, S.; Hinshaw, J. A.; Zaritskaya, L.; Williams, M. S. *Free Radical Biol. Med.* **2003**, *35*, 648.
27. Shimizu, S.; Narita, M.; Tsujimoto, Y. *Nature* **1999**, *399*, 483.
28. Lopez, E.; Ferrer, I. *Brain Res. Mol. Brain Res.* **2000**, *85*, 61.
29. Guo, Y.; Srinivasula, S. M.; Druilhe, A.; Fernandes-Alnemri, T.; Alnemri, E. S. *J. Biol. Chem.* **2002**, *277*, 13430.
30. Levites, Y.; Amit, T.; Mandel, S.; Youdim, M. B. *FASEB J.* **2003**, *17*, 952.
31. Park, C.; So, H. S.; Shin, C. H.; Baek, S. H.; Moon, B. S.; Shin, S. H.; Lee, H. S.; Lee, D. W.; Park, R. *Biochem. Pharmacol.* **2003**, *66*, 1287.
32. Bastianetto, S.; Zheng, W. H.; Quirion, R. *Br. J. Pharmacol.* **2000**, *131*, 711.
33. Ellis, G. H. *J. Assoc. Agric. Chem.* **1949**, *32*, 287.

Journal of Reproduction and Development, Vol. 50, No. 6, 2004

—Original—

Long-Term Treatment Effects of *Pueraria mirifica* Phytoestrogens on Parathyroid Hormone and Calcium Levels in Aged Menopausal Cynomolgus Monkeys

Hataitip TRISOMBOON[1,2], Suchinda MALAIVIJITNOND[2], Juri SUZUKI[3], Yuzuru HAMADA[3], Gen WATANABE[4,5] and Kazuyoshi TAYA[4,5]

[1]Biological Science Ph.D. Program, Faculty of Science, Chulalongkorn University, Bangkok 10330, [2]Primate Research Unit, Department of Biology, Faculty of Science, Chulalongkorn University, Bangkok 10330, Thailand, [3]Primate Research Institute, Kyoto University, Inuyama, Aichi 484-8506, [4]Laboratory of Veterinary Physiology, Tokyo University of Agriculture and Technology, Tokyo 183-8509, [5]Department of Basic Veterinary Science, The United Graduate School of Veterinary Science, Gifu University, Gifu 501-1193, Japan

Abstract. To determine the effect of *Pueraria mirifica* (PM) on serum parathyroid hormone (PTH) and calcium levels on aged menopausal monkeys (*Macaca fascicularis*), subjects were treated with 10, 100, or 1,000 mg/day of PM. Blood samples were collected every 5 days for 30, 90, and 60 days during pre-treatment, treatment, and post-treatment periods, respectively. Sera were assayed for PTH, estradiol, and calcium levels. PM-1,000 had the strongest effect on the decrease in PTH ($0.001<P\leq0.05$) and calcium levels ($0.001<P\leq 0.03$) during the treatment period. PTH levels remained low for the first 15 days of the post-treatment period ($0.01\leq P\leq0.05$). PM-10 induced a significant decrease in PTH level on day 80 ($P=0.02$) during the treatment period and a significant decrease in calcium level on day 75 ($P<0.01$). There were no changes in serum PTH and calcium levels throughout the study period in the PM-100 group. Estradiol levels decreased significantly during the treatment period in all treatment groups. The results suggest that long-term treatment with 1,000 mg/day of PM decreases serum PTH and calcium levels in aged menopausal monkeys, indicating that PM ameliorates bone loss caused by estrogen deficiency.

Key words: *Pueraria mirifica*, Phytoestrogen, PTH, Calcium, Aged menopausal monkey

(J. Reprod. Dev. 50: 639–645, 2004)

Menopausal osteoporosis is a disorder of the bone characterized by the progressive loss of bone tissue, and is caused by estrogen deficiency in both natural and surgical menopause [1]. Increased parathyroid hormone (PTH) secretion contributes to an increase in bone resorption and osteoporosis, which is related to estrogen deficiency [2, 3]. Although the exact mechanism has not been elucidated yet, PTH is a major factor involved in the systemic regulation of bone resorption. Overproduction of PTH leads to an increase in bone resorption compared with bone formation and contributes to general skeletal demineralization. Increased PTH levels have been found to be concomitant with decreased bone mass in aging people [4]. One pathogenetic mechanism of osteoporosis involves chronic loss of calcium balance caused by intestinal and renal calcium handling. This mechanism is characterized by an increase in PTH concentration, and is generally though to be a secondary response to a small

Accepted for publication: August 17, 2004
Correspondence: S. Malaivijitnond
(e-mail address: Suchinda.M@chula.ac.th)

reduction of serum calcium levels.

Several recent reports have indicated that soy, a rich source of isoflavone genistein and daidzein, has a beneficial effect, reducing bone loss associated with ovarian hormone deficiency [5–7]. Soy isoflavone treatment induced a large increase in bone mineral density (BMD) in ovariectomized rats [8] and mice [5]. Postmenopausal women with habitually high intakes of dietary isoflavones had significantly lower levels of serum PTH and higher BMD [6]. In an *in vitro* study, the decrease in bone calcium content induced by bone resorbing factors, PTH, and prostaglandins E_2 was inhibited completely by genistein [9]. Moreover, genistein blocked both the inactivation of acid phosphatase and the activation of alkaline phosphatase due to PTH in bone tissue, resulting in reduced bone resorption in rats [10]. The evidence strongly suggests that phytoestrogens play a role in preventing bone loss caused by estrogen deficiency in women as well as female animals, possibly through the reduction of PTH levels.

Pueraria mirifica (PM), known as White Kwao Krua, is an indigenous Thai plant that has long been used as a rejuvenating drug. The chemical content of its tuberous roots has been analyzed by high performance liquid chromatography and many phytoestrogenic substances were found, including miroestrol [11, 12], deoxymiroestrol, kwakhurin [13], coumestrol, and isoflavones (genistein and daidzein) [14, 15]. Several investigators have studied PM's estrogenic effect on the reproductive organs and their functions [16–18]. Prior research found a PM effect using an animal model [16–18]. Treatment with a suspension of PM at various doses influenced serum gonadotropin levels in both aged menopausal and adult cyclic cynomolgus monkeys [18, 19]. One study found that administration of crude extract of PM improved menopause-related symptoms in women such as hot flushes, frustration, sleep disorder, skin dryness, high blood cholesterol, and amenorrhea with no change in blood cells, or liver or renal functions [20]. No research, however, has studied the effects of PM on bone, calcium, or PTH levels. This is of interest for female animals and menopausal women who face bone disorder problems. The aim of this study, therefore, was to investigate the estrogenic effect of long-term treatment of PM on serum levels of PTH and calcium in aged menopausal monkeys. Aged menopausal cynomolgus monkeys were used in this study as a representative of menopausal women, because the physiological systems of cynomolgus monkeys, including hormonal patterns and reproductive function, are similar to those of humans [21, 22].

Materials and Methods

Animals

Aged menopausal monkeys (*Macaca fascicularis*, n=9) with a complete cessation of menstruation for at least one year, age more than 25 years, and weighing from 4.0–6.5 kg, were selected. The menopausal state of the monkeys was confirmed and checked daily by vaginal swabbing before and during treatment. The monkeys were housed separately in individual cages at the Primate Research Unit, Department of Biology, Faculty of Science, Chulalongkorn University, Bangkok, Thailand. Lighting conditions in the animal room were controlled (12:12 h light to dark cycle). Temperature and humidity fluctuated slightly depending on the season. The monkeys were fed daily with monkey chow (Pokaphan Animal Feed Co., Ltd., Bangkok, Thailand) in the morning (09:00–10:00 h) and were given fresh fruits in the afternoon (14:00–15:00 h). The experimental protocol was approved by the ethics committee in accordance with the guide for the care and use of laboratory animals prepared by the Primate Research Unit, Chulalongkorn University.

Experimental design

The nine aged menopausal monkeys were divided into three groups. The monkeys in each group (n=3) were fed daily with a suspension of PM at doses of 10, 100, or 1,000 mg/individual/day between 08:00–08:30 h. (hereafter abbreviated as PM-10, PM-100, and PM-1,000) The treatment schedule was separated into 3 periods: pre-treatment, treatment, and post-treatment for 30, 90, and 60 days, respectively. During the pre-treatment and post-treatment periods, monkeys were fed with 5 ml of distilled water. Blood samples, 3 ml, were collected from the femoral vein without anesthetization between 08:30–09:30 h every 5 days, then centrifuged 1,700 × g at 4 C, for 20 minutes and stored at –20 C until PTH, estradiol, and calcium were assayed.

P. mirifica suspension preparation

The fresh tuberous roots of PM were sliced, desiccated in a hot air oven at 70 C, and subsequently ground into 100 mesh powder. Then, the powdered stock was kept in a dark desiccator until preparation of the suspension with distilled water. The PM suspension was kept in a dark bottle at 4 C until feeding time

Hormonal analyses

Serum total calcium levels were measured by an atomic absorption spectrophotometer (AAS) according the method of Zettner and Seligson using a Roche/Hitachi system [23]. After extraction with ether, the serum level of estradiol was determined by RIA with ^{3}H-labeled radioligands as described by the established method of the World Health Organization (WHO) [24]. Serum PTH levels was assayed by a PTH-C radioimmunoassay kit (Eiken Chemical Co.Ltd. Bunkyo-ku, Tokyo, Japan). The procedure of the PTH assay and parallel checks were described in a previous report [25].

Statistical analysis

Serum levels of hormones were expressed as mean ± S.E.M. Analysis of variance (ANOVA) followed by the LSD test was applied to determine the significance of difference among the three periods of the experiment, and among the three groups. Differences were considered significant at $P<0.05$.

Results

Characteristics of hormonal pattern in aged menopausal monkeys

The menopausal state of the monkeys was confirmed by lower levels of serum estradiol (14.71 ± 1.18 pg/ml) and higher levels of LH (5.85 ± 0.80 ng/ml) compared to normal cyclic monkeys in the early follicular phase of the menstrual cycle in our

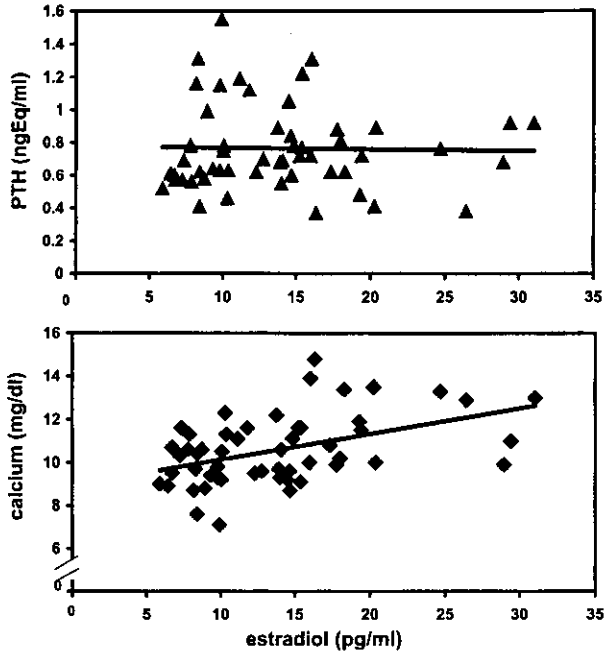

Fig. 1. Relationship between basal serum levels of PTH and calcium with estradiol in aged menopausal monkeys.

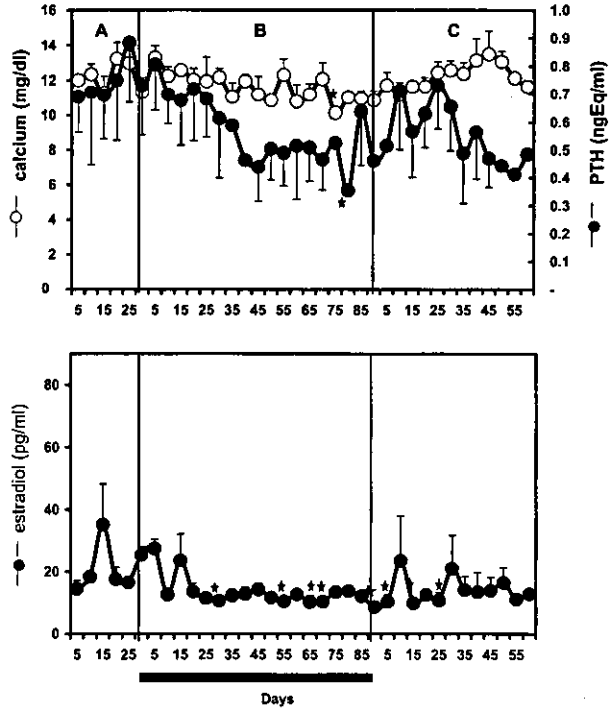

Fig. 2. Changes in serum PTH, calcium, and estradiol levels during the pre-treatment (A), treatment (B), and post-treatment (C) periods in monkeys treated with PM-10 (n=3). The horizontal bar indicates the treatment period. Stars show significant differences compared to pre-treatment levels ($P<0.05$).

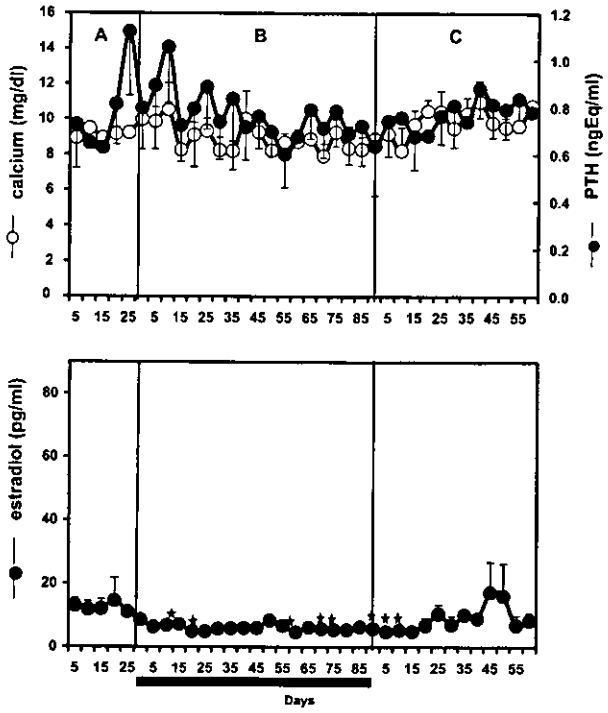

Fig. 3. Changes in serum PTH, calcium, and estradiol levels during the pre-treatment (A), treatment (B), and post-treatment (C) periods in monkeys treated with PM-100 (n=3). The horizontal bar indicates the treatment period. Stars show significant differences compared to pre-treatment levels ($P<0.05$).

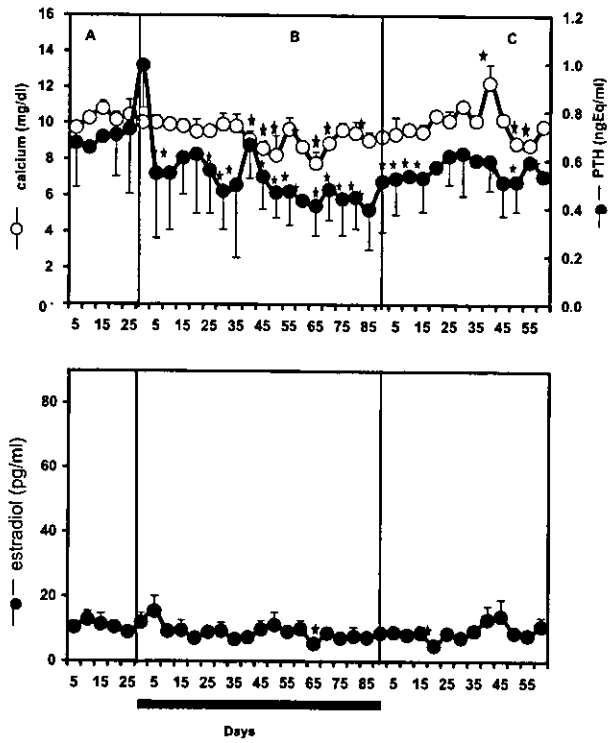

Fig. 4. Changes in serum PTH, calcium, and estradiol levels during the pre-treatment (A), treatment (B), and post-treatment (C) periods in monkeys treated with PM-1,000 (n=3). The horizontal bar indicates the treatment period. Stars show significant differences compared to pre-treatment levels ($P<0.05$).

colony (27.54 ± 4.31 pg/ml for estradiol and 0.51 ± 0.03 ng/ml for LH, unpublished data). Figure 1 shows the relationship between basal levels of estradiol and PTH as well as calcium. There was a slight positive correlation between the basal levels of calcium and estradiol ($r=0.46$, $P=0.001$), but no correlation between the levels of PTH and estradiol ($r=-0.02$, $P=0.88$).

Changes in serum PTH, calcium, and estradiol levels in monkeys treated with PM

Changes in serum PTH, calcium, and estradiol levels during the pre-treatment, treatment, and post-treatment periods in monkeys treated with PM-10, PM-100, and PM-1,000 are shown in Figs. 2–4. As shown in Fig. 2, monkeys treated with PM-10 showed a trend, but not significant, for the PTH level to become lower on days 40–90 ($0.06 \leq P \leq 0.51$) in the treatment period, than that in the pre-treatment period, except day 80 ($P=0.02$). After the cessation of PM treatment, the PTH level was quickly returned to the pre-treatment levels. Serum calcium levels decreased significantly on day 75 ($P=0.01$) during the treatment period but gradually returned to the basal levels thereafter. Serum estradiol levels significantly but sporadically decreased (days 30, 55, 65, 70, and 90 during the treatment period; $0.01<P<0.047$, and days 5, 15, and 25 during the post-treatment period; $0.04<P<0.05$).

As shown in Fig. 3, monkeys treated with PM-100 did not have significantly changed PTH and calcium levels throughout the study period. Estradiol levels decreased significantly at some points during the treatment (days 15, 20, 55, 70, 75, and day 90; $0.03<P<0.05$) and post-treatment periods (days 5 and 10; $0.03<P<0.05$) compared to the pre-treatment levels.

As shown in Fig. 4, monkeys treated with PM-1,000 showed a significant decrease in PTH levels during the treatment ($0.001<P<0.05$) compared to

the pre-treatment levels. PTH levels remained low for the first 15 days of the post-treatment period ($0.01<P<0.05$). Calcium levels decreased significantly only in the latter half of treatment period ($0.001<P\leq0.03$) and returned to the pre-treatment levels during the early post-treatment period. Estradiol levels were significantly lower than the pre-treatment levels on day 65 ($P=0.03$) of the treatment period and on day 20 ($P=0.01$) of the post-treatment period.

Discussion

Healthy menopausal monkeys have low levels of serum estradiol and there is a positive correlation between estradiol levels and calcium levels in their serum. It has been proposed that changes in estradiol levels influence intestinal calcium absorption and increase serum calcium levels as found in healthy humans [26]. However, we did not find the correlation between estradiol levels and PTH levels because of vary estradiol levels.

Our study is the first to report on the effect of phytoestrogens from the medicinal plant, PM, on altering serum levels of PTH and calcium in estrogen deficient animals. The results clearly demonstrate that aged menopausal monkeys treated with PM had reduced in PTH levels which were followed by a decline in serum calcium levels. The highest dose (PM-1,000) seems to have been more effective for the decrease of PTH and calcium levels than the lowest dose (PM-10). The effect, however, did not depend on dose, because a significant decrease was not observed in the PM-100 group. The reason why there was no effect of PM-100 on serum PTH and calcium levels in this study remains unknown.

Similar to our result, post-menopausal women consuming high isoflavones from a soy diet had lower levels of serum PTH [6]. The decrease of PTH levels was associated with increased BMD in the lumbar spine and Ward's triangle, suggesting that high intake of phytoestrogens may help to improve the state of hyperparathyroidism in postmenopausal women resulting in both lower rates of bone turnover and bone loss [6].

Estrogen administrations have been demonstrated to decrease serum levels of PTH and calcium in postmenopausal women [27, 28]. It has been suggested that estrogen directly inhibits bone resorption, leading to a decrease in calcium release from the bone into the blood circulation [27, 28]. Estrogen may have a direct action on enhancing intestinal and renal tubular calcium absorption and modulating calcium homeostasis [29]. In addition, an *in vitro* study showed that estrogen receptor (ER) was found in parathyroid cells, and estradiol, treatment caused a decrease in their basal DNA synthesis [30], suggesting that estrogen may have a direct effect on PTH secretion.

We consider that phytoestrogens in *P. mirifica* behave as an estrogen and decrease the PTH levels, since phytoestrogens compete with estradiol to bind to estrogen receptors, which are found in the renal, gastrointestinal tract, and bone [31, 32]. Phytoestrogens may effect these organs, improving calcium absorption, resulting in a secondary decrease in the PTH level. Based on the findings of Wong *et al.* [30] described above, we hypothesize that PM phytoestrogens have a direct action on decreasing PTH secretion from the parathyroid gland.

It is known that the mechanism of PTH in regulating calcium balance is very complex. Normally, it acts directly on the bone and kidney to increase calcium influx into the blood circulation. It also stimulates indirectly calcium absorption by the intestine. The overall effect of PTH is to increase the circulating calcium level [2]. Administration of PTH increased the serum calcium level in patients with hypoparathyroidism [33]. Low levels of serum PTH induced a reduction of serum calcium level in the blood circulation [2]. The results of the present study show that long-term treatment with PM can suppress the serum PTH level, followed by a decrease in the serum calcium level.

Although the long-term treatment of PM led to a decrease in serum calcium, serum calcium levels during the treatment period in all monkey groups (9.91 ± 0.13 mg/dl) stayed in a narrow range and remained within the normal range (10.57 ± 0.22 mg/dl) of aged monkeys. After the cessation of PM treatment, serum calcium levels returned to the pre-treatment level. Calcium is of fundamental importance to all biological activities, and it is also a vital component, not only in the mechanism of hormone secretion, but also in hormone action and is involved in neurotransmission and muscle contraction. For this reason, it is vital that the serum calcium concentration is kept within a narrow range. The fact that aged monkeys treated

with PM for 90 days, did not have greatly lowered serum calcium levels outside their normal range, means that the long-term treatment of PM, which contains phytoestrogens, does not have an adverse effect on calcium homeostasis in the physiological system.

Although our study cannot completely explain the mechanism of PM on the decrease of PTH and calcium levels, at the very least it can be said that the effects on PTH and calcium levels were not caused by endogenous ovarian estradiol but by PM phytoestrogens. This was confirmed by the low estradiol levels seen throughout the study period in all monkey groups. During PM treatment, serum estradiol levels were even lower than those in the pre-treatment period, which is considered to have been caused by a reduction in peripheral conversion of estrone and testosterone to estradiol. Previous reports showed that both genistein and coumestrol reduced conversion of estrone to estradiol [34, 35], and of androstenedione and testosterone to estradiol in human granulosa luteal cells [36].

In summary, the long-term treatment of 1,000 mg/day of PM can decrease the serum levels of PTH and calcium in aged menopausal monkeys. The present study suggests that 1,000 mg/day of PM has a beneficial effect on preservation of calcium content in the bone by reducing PTH secretion. However, to determine the appropriate dose of PM to reduce bone loss in menopausal women additional studies are necessary.

Acknowledgments

This work was supported by The Thailand Research Fund (TRF) contract no. PHD/0014/2544 for the Royal Golden Jubilee Program, (RGJ network) and no. BGJ/15/2544, Chulalongkorn University Research Grant and a Grant-in-Aid for Scientific Research (The 21st Century Center-of-Excellence-Program, E-I) from the Ministry of Education, Culture, Sports, Science and Technology of Japan.

References

1. **Pacifici R.** Editorial: cytokines, estrogen and postmenopausal osteoporosis–the second decade. *Endocrinology* 1988; 139: 2659–2661.
2. **Silverberg SJ, Bilezikian JP.** Parathyroid function and responsiveness in osteoporosis. In: Bilezikian JP, Marcus R, Levine MA (eds.), The Parathyroid Basic and Clinical Concepts. New York: Raven Press; 1994: 805–812.
3. **McKane WR, Khosla S, Risteli J, Robins SP, Muhs JM, Riggs BL.** Role of estrogen deficiency in pathogenesis of secondary hyperparathyroidism and increased bone resorption in elderly women. *Proc Assoc Am Physicians* 1997; 109: 174–180.
4. **Delmas PD, Stenner D, Wahner HW, Mann KG, Riggs BL.** Increase in serum bone gamma-carboxyglutamic acid protein with aging in women. Implications for the mechanism of age-related bone loss. *J Clin Invest* 1983; 71: 1316–1321.
5. **Ishimi Y, Miyaura C, Ohmura M, Onoe Y, Sato T, Uchiyama Y, Ito M, Wang X, Suda, T, Ikegami S.** Selective effects of genistein, a soybean isoflavone, on B-lymphopoiesis and bone loss caused by estrogen deficiency. *Endocrinology* 1999; 140: 1893–1900.
6. **Mei J, Yeung SSC, Kung AWC.** High dietary phytoestrogen intake is associated with higher bone mineral density in postmenopausal but not premenopausal women. *J Clin Endocrinol Metab* 2001; 86: 5217–5221.
7. **Yamori Y, Moriguchi E, Teramoto T, Miura MS, Fukui Y, Honda, K, Fukui M, Nara Y, Taira, K, Moriguchi Y.** Soybean isoflavones reduce postmenopausal bone resorption in female Japanese immigrants in Brazil: A Ten-week study. *J Am Coll Nutr* 2002; 21: 560–563.
8. **Blum SC, Heaton SN, Bowman BM, Hegsted M, Miller SC.** Dietary soy protein maintains some indices of bone mineral density and bone formation in aged ovarictomized rats. *J Nutr* 2003; 133: 1244–1249.
9. **Gao YH, Yamaguchi M.** Inhibitory effect of genistein on osteroclast-like cell formation in mouse marrow cultures. *Biochem Pharmacol* 1999; 58: 767–772.
10. **Yamaguchi M, Gao YH.** Inhibitory effect of genistein on bone resorption in tissue culture. *Biochem Pharmacol* 1998; 55: 71–76.
11. **Pope GS, Grundy HM, Jones HEM, Tait SAS.** The estrogenic substance (miroestrol) from the tuberous roots of *Pueraria mirifica*. *J Endocrinol* 1958; 17: 15–16.
12. **Jones HEH, Pope GS.** A study of the action of miroestrol and other oestrogens on the reproductive tract of the immature female mouse. *J Endocrinol* 1960; 20: 229–235.

13. **Chansakaow S, Ishikawa T, Seki H, Sekine K, Okada M, Chaichantipyuth C.** Identification of deoxymiroestrol as the actual rejuvenating principle of "kwao keur" *Pueraria mirifica*. The known miroestrol may be an artifact. *J Nat Prod* 2000; 63: 173–175.
14. **Ingham JL, Tahara S, Dziedzic SZ.** Coumestans from the roots of *Pueraria mirifica*. *Z Naturforsch* 1988; 43c: 5–10.
15. **Ingham JL, Tahara S, Dziedzic SZ.** Minor isoflavones from the roots of *Pueraria mirifica*. *Z Naturforsch* 1989; 44c: 724–726.
16. **Smitasiri Y, Junyatum U, Songjitsawad A, Sripromma P, Trisrisilp S, Anuntalabhochai S.** Postcoital antifertility effects of *Pueraria mirifica* in rats. *J Sci Fac CMU* 1986; 13: 19–28.
17. **Smitarsiri Y, Pangjit S, Anuntalabhochai S.** Inhibition of lactation in lactating rats with *Pueraria mirifica* compared with estrogen. *J Sci Fac CMU* 1989; 16: 7–11.
18. **Trisomboon H, Malaivijitnond S, Watanabe G, Taya K.** Estrogenic effects of *Pueraria mirifica* on the menstrual cycle and hormones related ovarian functions in cyclic female cynomolgus monkeys. *J Pharmacol Sci* 2004; 94: 51–54.
19. **Trisomboon H, Malaivijitnond S, Taya K, Watanabe G, Suzuki J.** Potential role of *Pueraria mirifica* on reproductive hormones in aged female cynomolgus monkeys. In: 4th Intercongress Symposium of the Asia and Oceania Society for Comparative Endocrinology; 2002; 4: 0–19.
20. **Muangman V, Cherdshewasart W.** Clinical Trial of the phytoestrogen-rich herb, *Pueraria mirifica* as a crude drug in the treatment of symptoms in menopausal women. *Siriraj Hosp Gaz* 2001; 53: 300–309.
21. **Malaivijinond S, Varavudhi P.** Evidence for morphine-induced galactorrhea in male cynomolgus monkeys. *J Med Primatol* 1998; 27: 1–9.
22. **Krajewski SJ, Abel TW, Voytko ML, Rance NE.** Ovarian steroids differentially modulate the gene expression of gonadotropin-releasing hormone neuronal subtypes in the ovariectomized cynomolgus monkey. *J Clin Endocrinol Metab* 2003; 88: 665–662.
23. **Zettmer A, Seligson D.** Application of atomic absorption spectrophotometery in the determination of calcium in serum. *Clin Chem* 1964; 10: 869–890.
24. **Sufi SB, Donaldson A, Jeffcoate SL.** WHO matched reagent program method manual. In: WHO collaborating center for immunoassay; 1983; London.
25. **Malaivijitnond S, Trisomboon H, Cherdshewasart W, Juri S, Yuzuru H, Kikuchi Y, Takenaka O.** Changes of aged related factors in various age of cynomolgus monkeys and after treated with *Pueraria mirifica* phytoestrogens. In: COE International Symposium Development and Aging of Primates; 2000; 68.
26. **Fujusawa Y, Kida K, Matsuda H.** Role of change in vitamin D metabolism with age in calcium and phosphorus metabolism in normal human subjects. *J Clin Endocrinol Metab* 1984: 7119–7226.
27. **Stock JL, Coderre JA, Mallette LE.** Effects of a short course of estrogen on mineral metabolism in postmenopausal women. *J Clin Endocrinol Metab* 1985; 61: 596–600.
28. **Khosla S, Atkinson EJ, Melton LJ, Riggs BL.** Effects of age and estrogen status on serum parathyroid hormone levels and biochemical markers of bone turnover in women: a population-based study. *J Clin Endocrinol Metab* 1997; 82: 1522–1527.
29. **Vincent A, Riggs BL, Atkinson EJ, Oberg AL, Khosla S.** Effect of estrogen replacement therapy on parathyroid hormone secretion in elderly postmenopausal women. *Menopause* 2003; 10: 165–171.
30. **Wong C, Lai T, Hilly JM, Stewart CEH, Farndon JR.** Selective estrogen receptor modulators inhibit the effects of insulin-like growth factors in hyperparathyroidism. *Surgery* 2002; 132: 998–1007.
31. **Onoe Y, Miyaura C, Ohta H, Nozawa S, Suda T.** Expression of estrogen receptor β in rat bone. *Endocrinology* 1997; 138: 4509–4512.
32. **Gustafsson J.** Estrogen receptor β-a new dimension in estrogen mechanism of action. *J Endocrinol* 1999; 163: 379–383.
33. **Winner KK, Yanovski JA, Sarani B, Cutler GB.** A randomized, cross-over trial of once-daily versus twice-daily parathyroid hormone 1–34 in treatment of hypoparathyroidism. *J Clin Endocrinol Metab* 1998; 83: 3480–3486.
34. **Makela S, Poutanen M, Lehtimaki J, Kostian ML, Santti R, Vihko R.** Estrogen-specific 17 beta-hydroxysteroid oxidoreductase type 1 (E.C. 1.1.1.62) as a possible target for the action of phytoestrogens. *Proc Soc Exp Biol Med* 1995; 208: 51–59.
35. **Whitehead SA, Cross JE, Burden C, Lacey M.** Acute and chronic effects of genistein, tyrphostin and lavendustin A on steroid synthesis in luteinized human granulosa cells. *Hum Reprod* 2002; 17: 589–594.

Exp. Anim. 54(1), 101–105, 2005

—Note—

Malignant NK/T-Cell Lymphoma Associated with Simian Epstein-Barr Virus Infection in a Japanese Macaque (Macaca fuscata)

Juri SUZUKI[1], Shunji GOTO[1], Akino KATO[1], Chihiro HASHIMOTO[1], Norikatsu MIWA[1], Satomi TAKAO[2], Takafumi ISHIDA[2], Ayumi FUKUOKA[3], Hiroyuki NAKAYAMA[3], Kunio DOI[3], and Koichi ISOWA[4]

[1]*Primate Research Institute, Kyoto University, Inuyama, Aichi 484-8506,* [2]*Graduate School of Science, University of Tokyo, Bunkyo, Tokyo 113-0033,* [3]*Graduate School of Agricultural and Life Sciences, University of Tokyo, Bunkyo, Tokyo 113-8657, and* [4]*Japan Bioscience Center Co., Ltd., Kaizu, Gifu 503-0628, Japan*

Abstract: *A case of spontaneous malignant lymphoma in a Japanese macaque (*Macaca fuscata*) was pathologically, etiologically and virologically studied. Nasal cavity was involved in the neoplastic lesions in addition to lymphoid and visceral tissues. Histopathological analyses revealed the presence of neoplastic cells classified into histiocytic Hodgkin-like cells and Reed-Sternberg-like cells. Histiocytic Hodgkin-like cells were CD16+ and CD20+, and the CD16+ cells were also positive for simian Epstein-Barr virus (sEBV)-encoded early RNA transcripts. RS-like cells were negative for CD3, CD16 and CD20. Antibodies to early antigen of sEBV were detected, while antibodies to simian T-cell leukemia virus-1 were negative. The case may correspond to EBV-associated nasal type NK/T-cell lymphoma in humans rather than Hodgkin lymphoma.*

Key words: *Japanese macaques, malignant lymphoma, simian Epstein-Barr virus*

Malignant lymphomas are common neoplasms in non-human primates [1, 9, 30] as in humans. Classification of lymphomas in non-human primates, however, is based only on the morphological features. In humans, Hodgkin lymphoma is distinguished from non-Hodgkin lymphoma by the presence of Hodgkin cells (histiocytic neoplastic cells with noticeable nucleus) and/or multinucleated Reed-Sternberg (RS) cells [2] that are derived from B cells in the germinal center, and moreover by various neoplastic cell markers [7, 24]. Analyses of CD markers also help us to classify non-Hodgkin lymphoma in non-human primates and provide more information about the lymphomagenesis [3, 21, 22]. There has been so far only one report on lymphoma with CD marker analyses for the Japanese macaque (*Macaca fuscata*) [31]. However, histological and etiological information were lacking from that report and a systematic study on primate malignant lymphoma has been awaited.

Certain groups of viruses are tightly associated with

(Received 27 April, 2004 / Accepted 25 August, 2004)

Address corresponding: J. Suzuki, Center for Human Evolution Modeling Research, Primate Research Institute, Kyoto University, Inuyama, Aichi 484-8506, Japan

and participate in lymphomagenesis in non-human primates as well as in humans. Epstein-Barr virus (EBV) classified as a lymphocrypto gamma herpesvirus is an etiological agent of lymphoproliferative disorders including Burkitt's lymphoma and infectious mononucleosis in humans [26, 33]. Recent studies on malignant lymphoma have revealed that EBV contributes to the development of Hodgkin and non-Hodgkin lymphoma including T-cell lymphomas such as NK/T-cell lymphoma [4, 5]. Virus isolates relevant to human EBV have been found in non-human primates and are called simian EBV (sEBV) [18]. The sEBV is well known to play an important role in oncogenesis in macaques [16, 25], and 98% of Japanese macaques were seropositive for anti-sEBV viral capsid antigen (sEBV VCA) [11, 12]. One of the primate T-lymphotropic retroviruses, simian T-cell leukemia virus (STLV)-1, has the potential to develop T-cell lymphoma in baboons (*Papio spp.*) [10] and African green monkeys (*Cercopithecus aethiops*) [17], and about 30% of Japanese macaques have been reported to be seropositive for STLV-1 [13, 14].

Recently, a Japanese macaque in our colony was found to have developed a malignant lymphoma and subsequently died. We here report the histopathological, virological and etiological data of the case.

The macaque was born and reared at the Primate Research Institute of Kyoto University. The rearing conditions were described in detail in our previous report [28]. The animal was a male Japanese macaque aged 4.6 years (yrs) and belonged to the Arashiyama troop. Autopsy was performed immediately after the death. Tissues with gross lesions were fixed in 10% formalin solution, embedded in paraffin, sectioned at 5 μm, and stained with hematoxylin and eosin (HE) for histopathological observation.

Immunostaining was performed on paraffin-embedded sections of tissues using antibodies to human CD3 (PS1, Nichirei, Japan) for T-cells, CD16 (NCL-CD16, Novo castra, UK) for NK-cells and CD20 (L26, Nichirei, Japan) for B-cells, which had been confirmed cross-reactive with Japanese macaque's lymphoid antigens on paraffin-embedded sections. Positive signals were visualized by using a Dako LSAB2/HRP kit (DakoCytomation, Japan).

To confirm the presence of sEBV in tumor cells, *in situ* hybridization was performed on sections of tissues using fluorescein-conjugated oligonucleotides (5'-ATCTCCTCCCCAGCATAACCGCTAGGGCAG-3' and 5'-ACCCCCCTCTGTCCGTAACCTC-TAGGCTAG-3') complementary to the portions of the sEBV-encoded early RNA transcripts (sEBERs) that are actively transcribed in latently infected cells. Sections of tissues, axillary and inguinal lymph nodes, of a normal Japanese macaque were used as a control. Signals for sEBERs were visualized by Universal RNA ISH and a DIG-AP detection kit (Nichirei, Japan).

Infection with STLV-1 was monitored by the detection of specific antibody to STLV-1 with an indirect immunofluorescence method. The procedure has been described previously [13]. As for the sEBV infection status, the presence of anti-sEBV VCA antibody and anti-sEBV early antigen (sEA) antibody were used as markers for the sEBV infection and the possible presence of sEBV associated cell proliferative diseases, respectively [22]. P3HR-1 cells [8] treated with 4 mM n-butyric acid (Wako Chem., Japan) and 20 ng/m*l* 12-tetradecanoylphorbol-13-acetate (TPA) (Sigma, USA) for 48 h, and Raji cells [23] treated with 20 ng/m*l* TPA for 5 days were fixed with acetone and used as target antigens of sEBV VCA and sEA, respectively. Fluorescein isothiocyanate-conjugated goat antibody to human immunoglobulins (Medical & Biological Laboratories, Japan) was used to visualize a positive reaction under a fluorescence microscope. The procedure for the detection of plasma antibodies to sEBV VCA and sEA has been described in detail previously [11].

At 3.8 yrs of age, lameness of the left hind limb, high body temperature (39.3°C), increase in white blood cell count (25,600/mm^3) and high concentration of plasma C-reactive protein (CRP) (2.6 mg/dl) were observed. A mass in the left nasal cavity with hemorrhage and rhinorrhea, and swelling of the axial lymph nodes were found at 4.6 yrs of age. Severe anemia (RBC 289 $\times$ 10^4/mm^3, hemoglobin 6.2 g/dl, and hematocrit 22.5%), low platelet count (10 $\times$ 10^4/mm^3) and high CRP (3.3 mg/dl) and high alkaline phosphatase (1,537 unit/litter) levels were documented before death at the age of 4.6 yrs. A hemogram was not available in the present case.

Gross lesions were characterized by systemic swelling of various lymph nodes (30–70 mm in diameter), a neoplastic mass in the nasal cavity (30 $\times$ 15 $\times$ 15 mm) and splenomegaly (1,250 $\times$ 850 $\times$ 300 mm).

Histopathological findings of the lymph nodes in-